

Estimation of Liquid–Liquid–Vapor Equilibria Using Predictive EOS Models. 1. Carbon Dioxide–*n*-Alkanes

Ilya Polishuk,^{*,†} Jaime Wisniak,[†] and Hugo Segura[‡]

Department of Chemical Engineering, Ben-Gurion University of the Negev, Beer-Sheva, Israel,
and Department of Chemical Engineering, Universidad de Concepción, Concepción, Chile

Received: August 20, 2002; In Final Form: December 19, 2002

This study looks for the first time at the possibility of predicting liquid–liquid–vapor equilibria without preliminary resource to experimental data. For this purpose, the two most successful G^E -based semipredictive models (PSRK and LCVM) and the global phase diagram (klGPD)-based semi-predictive approach (GPDA) have been implemented and compared. Although G^E -based models require a significant amount of experimental data for evaluation of their parameters and prediction of the equilibrium, GPDA needs no more than 2–3 key experimental points. The superiority of GPDA, which considers the entire thermodynamic phase space, over the G^E -based models, which are based on the fit of VLE data, is clearly demonstrated. Although the G^E -based models fail to predict global phase behavior and to describe three-phase data accurately, GPDA yields exact predictions of the global phase behavior and accurate estimations of the composition and density of the vapor and the CO₂-rich phases. In addition, it is accurate in describing the P–T projection of three-phase lines. All of the models considered are unable to predict the hydrocarbon-rich phase accurately. Presently, this problem cannot be solved without violating the predictive character of the model.

1. Introduction

Investigation and prediction of phase behavior in mixtures is an important objective of modern physical chemistry. In real binary systems, three fluid phases can be present in equilibrium, however, the phase rule does not define them. For example, it has already been demonstrated¹ that binary systems theoretically may exhibit three liquid phases in equilibrium (LLLE); although some experimental results^{2,3} might be considered as an evidence for such behavior, LLLE has not been observed in practice yet.

Presently, liquid–liquid–vapor equilibrium (LLVE) is the only three-fluid phase equilibria known to exist in binary mixtures (Figure 1). LLVE may be present in all binary systems, excepting those which exhibit type I (according to classification of van Konynenburg and Scott⁴). Moreover, all other types of phase behavior are characterized by different shapes of LLVE. For example, type II involves low-temperature LLVE, which is restricted by an upper critical endpoint (UCEP) between L_1 and L_2 . UCEP of type III represents a merging of L_1 and the vapor phase (the so-called K point). Phase behavior of type IV includes two LLVE branches: the low-temperature branch of type II and another one restricted by both K point and the L_1 – L_2 lower critical endpoint (LCEP). Phase behavior of type V includes only the second LLVE branch of type IV. Type VI is characterized by LLVE restricted by two L_1 – L_2 critical endpoints. It can be seen then that LLVE is a central element of the phase diagram because it joins its two main parts (LLE and VLE) and defines the topology of phase behavior.

Thus, accurate description of three-phase equilibria should be considered a challenging task for modern thermodynamics. Although recent models allow a very good correlation of almost

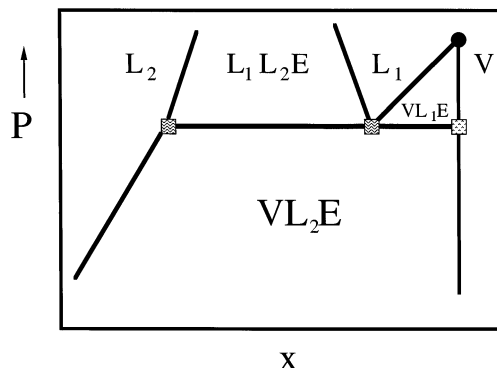


Figure 1. Schematic presentation of isotherm with LLVE.

every experimental data, including LLVE, it is obvious that prediction of data is much more important than their correlation. Nevertheless, prediction of three-phase equilibria without preliminary resource to experimental data of particular systems has not received suitable attention in the literature.

A very important contribution to LLVE modeling is that of Gregorowicz and de Loos,⁵ who proposed a useful procedure for finding UCEP and LCEP in mixtures, using equations of state (EOS). They also implemented the Redlich–Kwong–Soave⁶ (RKS) EOS and classical mixing rules with binary parameters set to zero and fitted to VLE, to predict the LLVE in several binary and ternary hydrocarbon systems. Their results are only in qualitative agreement with the experimental data for both sets of interaction parameters. Later on,⁷ it has been demonstrated that the EOS of Peng and Robinson⁸ (PR) with both classical and Wong–Sandler⁹ mixing rules yields similar results and also that the SAFT model¹⁰ is substantially less accurate than cubic EOSs.

Attempts to predict phase behavior in mixtures cannot be successfully done without recognizing the fact that all regions

* To whom correspondence should be addressed. Phone: +972-8-6461479. Fax: +972-8-6472916. E-mail: polishyk@bgumail.bgu.ac.il.

[†] Ben-Gurion University of the Negev.

[‡] Universidad de Concepción.

of the thermodynamic phase space are closely interrelated. In other words, one can hardly achieve accurate modeling of LLVE by fitting the binary parameters only to VLE data and neglecting LLE. This fact emphasizes a need of reexamination of the present methods of predicting phase equilibria, which are usually handled with the local fit of available data, and development of global approaches that consider an entire thermodynamic phase space.

Since van Konynenburg and Scott⁴ first introduced the idea of the global phase diagram (GPD), it has been intensively implemented in the investigation of different thermodynamic models. Recently,¹¹ a GPD in the projection of two binary parameters k_{12} and l_{12} (klGPD) was proposed as a device for the proper evaluation of the model parameters and shown to be a very effective tool for detecting fundamental regularities characteristic for phase equilibria generated by EOSs.¹²

Our approach is based on the fact that the configuration of VLE phase boundaries at any temperature is defined by (1) the position of the vapor-liquid critical point and (2) the distance from any particular temperature to the upper critical solution temperature (UCST) of the system, at which the homogeneous liquid-phase splits into two phases. This is because the inflections of bubble-point curves always change *continuously* from VLE to LLE. Hence, the accuracy in describing VLE is determined by the exactness with which the model predicts LLE, a fact which is not always evident when dealing with the local fit of data.¹² In other words, different kinds of phase equilibria, such as VLE and LLE, are interrelated not only *qualitatively* but also *quantitatively*.

Thus, it appears that an appropriate description of phase equilibria in the system can be achieved by the accurate correlation of only two experimental points that characterize VLE and LLE in the system, namely, the upper critical endpoint (UCEP) and the critical pressure maximum (CPM). In addition, it has been demonstrated that the experimental values of these key points in different homologues can be correlated by EOSs using the same values of the binary parameters k_{12} and l_{12} . In other words, each homologues series has its own characteristic balance between VLE and LLE. This observation has allowed us to formulate the novel semipredictive GPD-based approach (GPDA) involving estimation of the binary interaction parameters for a certain homologue using klGPD, with further implementation for predicting the data of other homologues.¹² Because this approach needs only 2–3 experimental points of one system in order to predict the entire thermodynamic phase space of the complete homologues series, it is advantageous over other widely used semipredictive approaches such as PSRK¹³ and LCVM,¹⁴ which require a large amount of data for evaluating their parameters.

In the present study, we examine for the first time the ability of these semipredictive approaches to estimate three-phase equilibria without preliminary resource to the pertinent experimental data. Here, we consider three-phase equilibria in the very important homologue series of carbon dioxide-*n*-alkanes. The data of this series are very difficult to predict because of the presence of a large quadrupole moment in the carbon dioxide molecule.¹⁵ Thus, the systems selected for this study present a challenging task for the semipredictive approaches, as shown below.

2. Theory

The present development of molecular theory does not allow an adequate evaluation of entirely predictive methods, which could be reliable for predicting data in mixtures. Therefore, the

usual practice is to develop semipredictive approaches that use some experimental data in order to predict the missing ones. It is widely agreed that models characterized by high correlative ability should also be good for predictive purposes. Accordingly, it is expected that cubic EOSs combined with Huron-Vidal type mixing rules, which have an excellent flexibility in correlating data, should exhibit good predictive ability. The predictive Soave-Redlich-Kwong (PSRK) EOS,¹³ which presents a combination of the modified RKS¹⁶ and the modified Huron-Vidal (MHV1) mixing rules,¹⁷ is considered among the most successful G^E -based models because it has the largest parameter matrix.^{18–20}

However, our previous studies^{21,22} contradict the widely accepted opinion regarding advantages of this model. It was demonstrated that the predictive ability of PSRK is usually overestimated and that its complex functionalities may have only a modest contribution to the accurate prediction of data. In particular, PSRK usually has a strong tendency to overestimate the liquid-liquid immiscibility range. In addition it predicts inaccurate results for asymmetric systems that have not been considered for evaluating its parameters. It seems that the latter procedure is responsible for the inaccurate predictions of PSRK because it is performed fitting only the VLE data and neglecting the other equilibrium data, such as LLE, LLVE, and critical lines. Attempts to correct the PSRK parameters in an artificial manner^{23–25} in order to improve the accuracy of predicting data in asymmetric systems, leads only to error propagation of the original improper data fit. Such practice leads to prediction of a nonphysical trend of the global phase behavior.²² Hence, these modifications will not be considered here.

An alternative to PSRK for predicting data in asymmetric systems is the linear combination of Vidal and Michelsen mixing rules (LCVM) model.¹⁴ It consists of the modified PR²⁶ and a mixing rule that presents an empirical combination of MHV1²⁰ and the original Huron-Vidal model.²⁷ The success of LCVM in describing VLE data in asymmetric systems has been recently²⁸ explained by the fact that LCVM diminishes the difference between the combinatorial terms of UNIFAC and the cubic EOS itself, which is characteristic of other G^E -based models. Nevertheless, we have proposed a different explanation for the superiority of LCVM over PSRK in predicting the data for asymmetric systems, namely, the significantly larger base of experimental data implemented by LCVM for the evaluation of its parameters. In the particular case of CO₂-*n*-alkanes, PSRK uses the data of homologues up to *n*-decane,¹³ and LCVM, up to *n*-octacosane.¹⁴ However, such practice does not remove the fundamental disadvantage of the model, whose parameters are obtained by an improper fit, namely, its low predictive ability.²²

It should also be realized that the complex and multidimensional nature of G^E -based models such as PSRK and LCVM significantly hinders the implementation of methodologies that consider the entire thermodynamic phase space instead of a VLE data fit. For this reason, we have implemented the klGPD methodology using the simplest classical mixing rules. In addition, it is well-known that both RKS^{6,16} and PR^{8,26} are inaccurate in predicting other properties such as liquid densities. Moreover, it has been shown that RKS^{6,16} and PR^{8,26} may generate undesirable numerical pitfalls, which are responsible for predicting nonphysical phase behavior in mixtures.^{29–30}

Thus, appreciation of the fact that all parts of the thermodynamic phase space are closely interrelated encourages the development of an equation of state, which would be simultaneously accurate for the largest number of properties and be

free of numerical pitfalls. Recently, we have proposed the following EOS that meets these requirements in a satisfactory manner:²²

$$P = \frac{RT(V_m + 0.125b)}{V_m(V_m - 0.875b)} - \frac{aT_r^{(m_1 T_r^{m_2})}}{(V_m + c)(V_m + d)} \quad (1)$$

where m_1 and m_2 are adjustable parameters for the appropriate presentation of the vapor pressure curve. The values of these parameters for light gases, for which high quality data are available, and for complex polar compounds should be evaluated separately (for CO_2 $m_1 = -0.33595$ and $m_2 = -0.15187$). For other compounds, the values of m_1 and m_2 can be generalized; for example, we have proposed that for *all* hydrocarbons m_2 be taken as 0.25 and for those having a carbon number larger than 10, by the following expression:

$$m_1 = \frac{-0.4162 + 1.5447\omega - 2.5285\omega^2 + 0.81466\omega^3}{b} \quad (2)$$

The values of a , b , c , and d are obtained solving the system of the four following equations:

$$\left(\frac{\partial P}{\partial V_m}\right)_{T_c} = \left(\frac{\partial^2 P}{\partial V_m^2}\right)_{T_c} = 0 \quad (3)$$

$$V_{m,c,\text{EOS}} = \xi V_{m,c,\text{EXPT}} \quad (4)$$

where ξ is a dimensionless number equal to $1 + V_{m,\text{triple point}}$

$$b = \frac{4}{3.5} V_{m,\text{triple point}} \quad (5)$$

For light gases and heavy substances having a carbon number larger than 10, eqs 4 and 5 consider the molar volume of the solid phase at the triple point, and for others, they consider the molar volume of the liquid phase. The system of eqs 3–5 is easily solved, and the pertinent numerical procedure has been already published.³¹

As already indicated, the parameters of eq 1 for mixtures are obtained using the following classical van der Waals mixing rules:

$$z = \sum_{ij} x_i x_j z_{ij} \quad (6)$$

where $z = a$, b , c , and d .

The cross-interaction parameters are obtained with the following combination rules:

$$\begin{aligned} a_{21} &= a_{12} = (1 - k_{12})\sqrt{a_{11}a_{22}} \\ b_{12} &= b_{21} = (1 - l_{12})\frac{b_{11} + b_{22}}{2} \\ c_{12} &= c_{21} = \frac{c_{11} + c_{22}}{2} \\ d_{12} &= d_{21} = \frac{d_{11} + d_{22}}{2} \end{aligned} \quad (7)$$

where k_{12} and l_{12} are binary adjustable parameters. Proper evaluation of their values is the objective of GPDA. Figure 2 schematically presents a typical kIGPD for an asymmetric system. The upper part of the diagram corresponds to weak cross-attraction forces, which result in absolute liquid–liquid

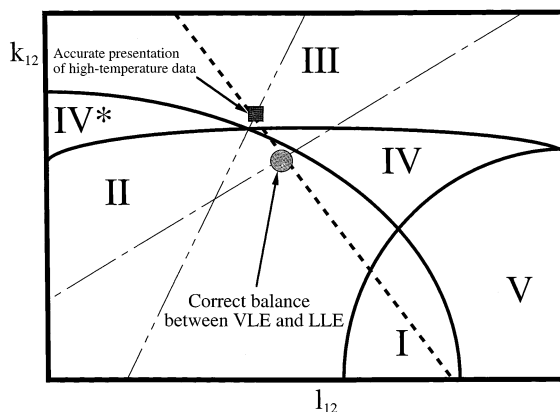


Figure 2. Schematic presentation of kIGPD in an asymmetric system. Fat solid lines, loci of TCP and DCEP that present the borders between the regions of types of phase behavior. Dashed line, locus of the experimental value of CPM. Dot–dashed line, locus of the experimental value of UCST. Dot–dot–dashed line, locus of the temperature at which CPM takes place.

immiscibility in a wide range of temperatures (phase behavior of type III). The range of this behavior is restricted by the double critical endpoint (DCEP) line, which separates it from the region of type IV, and by the tricritical point (TCP) line, which distinguishes between the regions of types III, IV, V, and I, II, IV*.

As explained before, kIGPD is a very useful tool not only for the general research of the topology of phase behavior, but also for the proper evaluation of the EOS parameters. This is because kIGPD allows presenting both qualitative and quantitative information about the system. In particular, kIGPD will show which values of the binary parameters should be used to correlate the experimental values of CPM and UCEP. In other words, the experimental values of these key points, which characterize the phase behavior of the system, can be traced in kIGPD as the loci of CPM and UCEP.

It should be realized that using two binary parameters makes it possible to correlate each particular property by every EOS. However, EOSs significantly differ in their ability to present several properties simultaneously. Therefore, the accuracy of models should be measured by their ability to generate intersections of the different property lines in the right places of kIGPD.

For example, PR and RKS are unable to generate the intersection of the two fundamental key property lines, namely, the CPM and UCEP loci of CO_2 –*n*-decane in the region of type II exhibited by this system.³¹ It should be realized that this intersection presents the most important point on the kIGPD because it corresponds to the correct balance between VLE and LLE in the system¹² (see Figure 2). Indeed, CPM presents a key point that characterizes the vapor–liquid equilibrium in the system. However, accurate presentation of CPM alone is not enough for an appropriate modeling of VLE in the system. The fact that all regions of the thermodynamic phase-space are closely interrelated explains why the shapes of bubble-point lines are defined by distance between them and the UCEP. Thus, location on the CPM isobar with the overestimated UCEP isotherm will give an accurate prediction of the critical points, but it will also underestimate the bubble point pressures and vice versa.¹² In other words, a pair of the binary adjustable parameters that represent the correct balance between VLE and LLE (and therefore allow the appropriate presentation of the entire thermodynamic phase space) is located at the intersection of the UCEP and CPM loci on kIGPD.

Because the kIGPDs of equations such as PR and RKS for the system CO₂–*n*-decane do not include the intersection of the UCEP and CPM loci, these equations cannot predict simultaneously the critical and the subcritical phase equilibria in this system and in the whole homologue series under consideration. Therefore, the solution to the problem should be addressed to more advanced models, such as eq 1, which are developed for the appropriate presentation of the kIGPD properties. Nevertheless, there are cases where even the latter models cannot achieve intersection of all key loci at one point. In particular, in asymmetric systems such as CO₂–*n*-decane, it is usually difficult to achieve the simultaneous intersection of loci that represent the experimental values of temperature and pressure of CPM together with the locus of UCEP. It should be understood that an exact presentation of the CPM temperature is responsible for the accurate presentation of high-temperature data. As discussed before,¹¹ the problem of the simultaneous intersection of different loci on kIGPD can be solved by attaching the binary parameter k_{12} with the appropriate temperature dependency.

It should be realized that every thermodynamic state or experimental value could be traced as a path in the kIGPD. However, properties not having a solid mathematical definition must be estimated by tedious trial-and-error procedures. Therefore states, which can be determined by solving algebraic equations, are more suitable for presentation in the kIGPD. Mathematical conditions for borders between types of phase behavior have been already discussed.^{1,11} The mathematical definition of the CPM in addition to the algebraic condition of every critical point

$$\left(\frac{\partial^2 G}{\partial x^2}\right) = \left(\frac{\partial^3 G}{\partial x^3}\right) = 0 \quad (8)$$

includes also the following expression

$$\left(\frac{\partial^3 G}{\partial x^2 \partial T}\right) = 0 \quad (9)$$

Hence, CPM is obtained by solving a system of three nonlinear equations. For the temperature locus of CPM, the three variables are composition, molar volume, and one of the binary parameters. Calculation of the CPM pressure locus is somewhat more complex because it requires converting the pressure to the molar volume using an EOS. The three variables are then composition, temperature, and one of the binary parameters.

The thermodynamic expression for the UCEP has been derived by Deiters and Pegg.¹ However, in the case of eq 1, the pertinent expression becomes somewhat complex, and the calculation of the UCEP loci follows a relatively tedious procedure. Nevertheless, the problem can be considerably simplified considering the fact that liquid–liquid critical lines usually do not exhibit a strong pressure dependency. Therefore, the UCEP locus almost overlaps with the locus that represents the zero-pressure critical reference state in the region of type II of kIGPD. A very simple expression for this state has been proposed recently.³²

Experience shows that the balance between VLE and LLE does not significantly change along a homologue series. In other words, intersection between the loci of CPM and UCEP, which is necessary for the appropriate and overall description of mixtures, usually takes place at similar values of k_{12} and l_{12} . This observation reveals the basis of the GPDA. Thus, to predict the entire thermodynamic phase space of a complete homologue series, it is necessary to know only the experimental value of

UCEP together with the pressure (and sometimes the temperature of CPM) of one of the homologues. It is helpful to consider as reference systems those homologues that exhibit the Type II behavior and which have been intensively investigated. In the series under consideration, the best candidate is the system CO₂–*n*-decane. Here, the binary parameters of the series have been evaluated using the kIGPD of this system.

The range of applicability of GPDA can be substantially enlarged if the values of the binary interaction parameters change proportionally to the values of the corresponding pure-compound parameters. Such proportionality can be easily established for the case of a linear combination rule for the covolume, as follows:

$$l_{12} = \frac{b_{22} - b_{11}}{b_{22} + b_{11}} L_{12} \quad (10)$$

where L_{12} is a value characteristic for a given homologues series.

The following proportional relation for the binary interaction parameter k_{12} , including the appropriate temperature dependency, has been developed:

$$k_{12} = \left(K_{11} - l_{12} \frac{T_{c2}}{T_{c1}}\right)(1 - t) + K_{22}t \quad (11)$$

where K_{11} and K_{22} are characteristic values for a given homologues series, and t is given by the following dimensionless functionality:

$$t = \tanh \left[\left(\frac{T - T_{c1}}{T_{c2}^* - T_{c1}} \right)^2 \right] \quad (12)$$

For homologues heavier than the reference homologue (CO₂–*n*-decane), $T_{c2}^* = T_{c2}$. For lighter homologues T_{c2}^* is equal to the T_{c2} of the reference homologue. Therefore, for all lighter homologues, T_{c2}^* will be taken as 617.7 K, the T_c of *n*-decane.³³ This will allow for the keeping of the same temperature dependency of k_{12} along the homologues series. For the series CO₂–alkanes, $K_{11} = 0.1$, $K_{22} = 0.35$, and $L_{12} = 0.02$.

We will now analyze the ability of PSRK, LCVm, and GPDA to predict the three-phase LLVE equilibria in homologue series under consideration.

3. Results and Discussion

It is not always easy to evaluate if the G^E -based models presented in the literature^{13–14,18–20,23–26} are predictive or correlative. This is due to the fact that a large amount of experimental VLE data has been used for evaluating the parameters of these models. In this respect the accuracy in modeling of three-phase data gives immediate evidence about their predictive ability because LLVE data has been usually not considered for the parameter fit.

However, some very important information regarding the characteristic features of the EOSs still can be studied analyzing their results for VLE. Thus, Figure 3 compares the experimental data of CO₂–*n*-tetradecane with those predicted by PSRK,¹³ LCVm,¹⁴ and GPDA at 344.3 K. Here, PSRK and GPDA appear as entirely predictive models because the data of the present system have not been used for evaluating their parameters. As usual, PSRK fails to predict the data because of overestimation of immiscibility. In contrast, GPDA predicts them with reasonable accuracy. Unlike the two latter equations, LCVm appears here as a correlative model. Hence, it does not seem surprising that it describes precisely the bubble-point data outside the

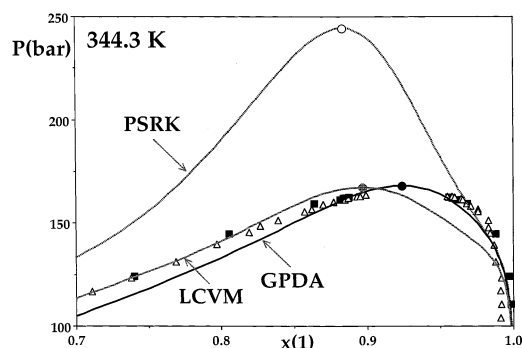


Figure 3. VLE in the system $\text{CO}_2(1)$ – n -tetradecane (2) at 344.3 K. Black solid line, data predicted by GPDA. Gray solid line, data predicted by LCVm. Black dot line, data predicted by PSRK. ●, gray dot, and ○: calculated critical points. Experimental data: ■, ref 34; △, ref 35.

critical region. However, this accuracy is achieved not by the reliable and robust character of the model but also by fitting of the pertinent VLE data. The latter approach tends to ignore the fact that all regions of the thermodynamic phase space are closely interrelated. As a result, LCVm significantly underestimates the composition of the critical point (see Figure 3).

Let us look how the underestimation of the critical compositions affects the ability of LCVm to predict LLVE. The only system for which the reliable data of both LLVE and the critical points are available is CO_2 – n -tridecane. In addition, this system belongs to transitional type IV, which attaches it with primary importance for the analysis of phase behavior. It can be seen (Figure 4) that the LCVm attribute of underestimating of critical composition increases as the LCEP is approached. As a result, it predicts inaccurately the composition of this key point. Because the composition of all critical endpoints are closely interrelated, the present location of the LCEP also moves down the composition of other critical endpoints. Therefore, LCVm also yields an inaccurate prediction of the UCEP and the related liquid phases. Moreover, underestimating the composition of the K point results in a longer critical line, which connects it with the critical point of pure carbon dioxide. Hence, this critical line rises to high pressure. In other words, underestimation of the composition of the K point causes overestimation of its pressure. It should be realized that the data of K points play a very important role in the design of supercritical extraction processes. Consequently, LCVm can hardly be considered as a reliable equation for modeling of the pertinent data.

K points are less flexible than other critical endpoints so that an inaccurate prediction of LCEP is mostly expressed in the enormously large range of compositions of the LLVE. As a result, all critical endpoints are dispersed far away one from the other and do not meet at the correct places, namely, at the experimental values of TCP and DCEP. Thus, in kGPDA, LCVm will fail in predicting the borders between regions of phase behavior, which are defined by these transitional states.²² In other words, neglecting parts of the thermodynamic phase space *always* carries a price: underestimation of the critical compositions in an attempt to achieve a precise fit of the bubble-point lines results in a very inaccurate description of the three-phase data. This, in turn, leads to failure in predicting the global phase behavior of the whole homologue series. PSRK again significantly overestimates the immiscibility, and thus, this model is both qualitatively and quantitatively inaccurate.

In contrast, GPDA is exact in predicting the topology of phase behavior and predicts the critical composition accurately. Consequently, it is also relatively accurate in predicting the critical endpoints, in describing L_1 , and in predicting the DCEP

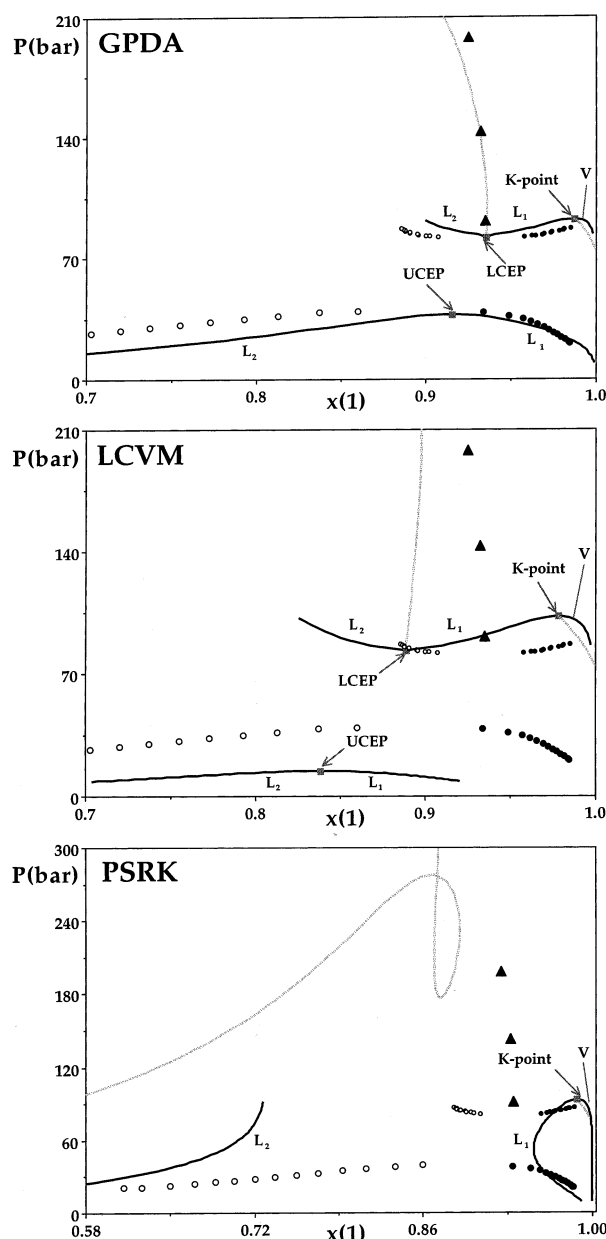


Figure 4. Phase equilibria in the system $\text{CO}_2(1)$ – n -tridecane(2). Black solid lines, predicted three-phase lines. Gray solid lines: predicted critical curves. Gray square: predicted critical endpoints. ▲, experimental critical data.³⁶ ●, experimental compositions of the CO_2 -rich phase (L_1).^{37–38} ○, experimental compositions of the hydrocarbon-rich phase (L_2).^{37–38}

and TCP.²² GPDA correctly reproduces the shape of LLVE between the K point and the LCEP, although it slightly overestimates its temperature. Recently,⁷ it has been demonstrated that such LLVE equilibria are very difficult to represent accurately, even when using the models that do not predict but correlate data. Thus, Figure 4 outlines the advantage of the approach that considers the entire thermodynamic phase space and not its separated parts. GPDA overestimates the content of CO_2 in the L_2 phase, because of its inability to describe the crossover behavior around the UCEP. Nevertheless, it should be concluded that GPDA produces a reasonable distribution of the inevitable deviations from the experimental data over the whole thermodynamic phase space and predicts these data in robust manner.

The regularities listed above allow a better understanding of the results predicted by the models under consideration for other

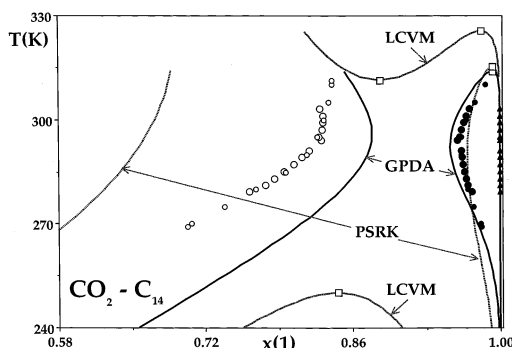


Figure 5. Compositions of LLVE equilibria in the system CO₂(1)–*n*-tetradecane(2). Black solid line: data predicted by GPDA. Gray solid line: data predicted by LCVM. Black dot line: data predicted by PSRK. □, calculated critical endpoints. ▲, experimental data of the vapor phase.³⁹ Experimental data of the CO₂-rich phase (L₁): ●³⁸ ●³⁹. Experimental data of the hydrocarbon-rich phase (L₂): ○³⁸ ○³⁹.

members of the homologue series. Let us consider again the CO₂–*n*-tetradecane system and examine the three-phase equilibria compositions in this system (Figure 5). It can be seen that LCVM completely fails to predict data, and as mentioned before, it significantly underestimates the compositions of the critical endpoints moving them away one from the other. Although in the present case LCEP and the L₁–L₂ UCEP slightly approach each other in comparison with the previous homologue, they are still far away. As a result, LCVM continues to predict phase behavior of type IV for a system that already exhibits phase behavior of type III. Moreover, LCVM continues to overestimate the pressure of the K point, a result, which is characteristic of this model. Consequently, LCVM predicts the three-phase split in the region of VLE and generates the homogeneous liquid phase where the experimental LLVE is located. In other words, there is no connection between the predictions of LCVM and the experimental three-phase data, a fact that reveals the price paid for the precise local fit of the bubble points (see Figure 3).

In contrast, the topology of phase behavior and the composition of the CO₂-rich phase (L₁) are predicted correctly by GPDA and PSRK. However, both of them fail to describe accurately the hydrocarbon-rich phase (L₂). PSRK significantly underestimates its composition because of its tendency to overestimate the immiscibility. Although GPDA is much more accurate than PSRK in describing this phase, it still overestimates its composition.

In the analysis of the previous homologue, this result has been related to the inability of the model to describe the crossover behavior, a fundamental drawback of all analytical equations. This inability becomes less meaningful when predicting the low-temperature VLE restricted by the pure compound vapor pressure points or by critical points with high content of solvent. However, it seriously affects the accuracy of the model in predicting phase equilibria with the critical points of middle and low content of solvent, which are characteristic for high-temperature VLE and the LLE. Decreasing the value of the binary parameter l_{12} is a very effective way to widen the LLE phase envelope. However, such a practice will not allow implementation of the kLGD methodology (see Figure 2). In other words, presently, we do not know how to predict precise results for all three phases in equilibrium without resource to experimental data.

Additional important information is presented in Figure 6, which examines the ability of the models to predict the volumetric data. Although GPDA and PSRK describe in a

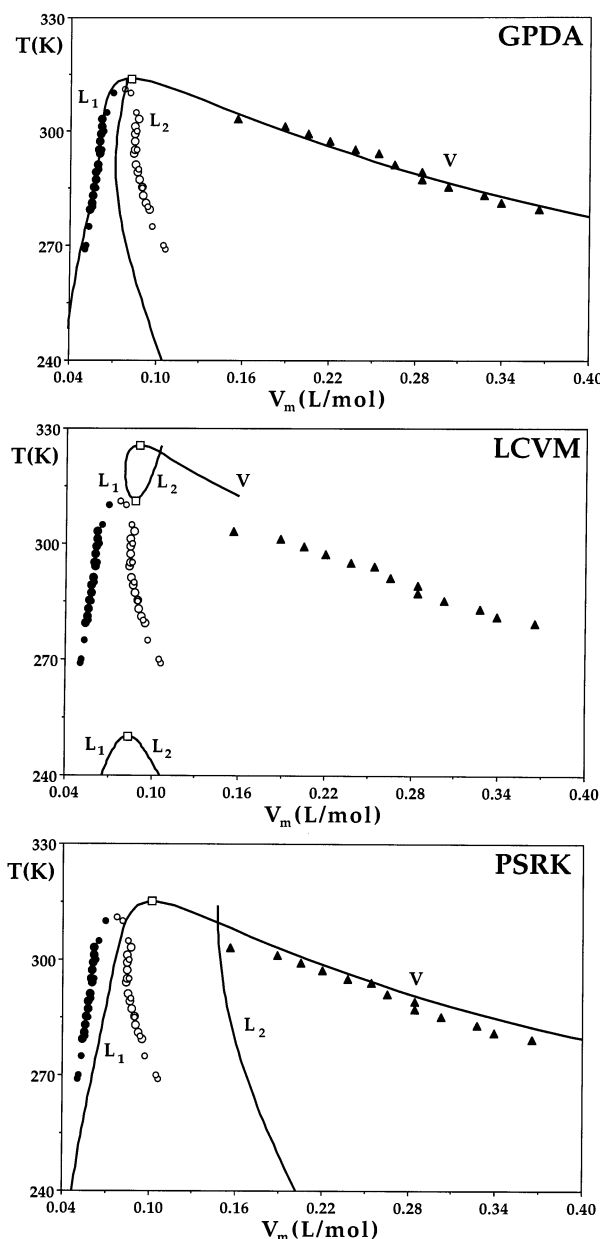


Figure 6. Molar volumes of LLVE equilibria in the system CO₂(1)–*n*-tetradecane(2). Black solid line: calculated data. □, calculated critical endpoints. ▲, experimental data of the vapor phase.³⁹ Experimental data of the CO₂-rich phase (L₁): ●³⁸ ●³⁹. Experimental data of the hydrocarbon-rich phase (L₂): ○³⁸ ○³⁹.

similar manner the compositions of the L₁ and V phases (Figure 5), they yield a substantially different prediction of the molar volumes. Although GPDA yields a precise prediction of the data, PSRK significantly overestimates them. This is because PSRK is based on the imperfect RKS,^{6,16} which overestimates the critical compressibility and the related volumetric data. In contrast to PSRK, GPDA is based on a four-parameter EOS (eq 1), which is optimal for representing volumetric properties. GPDA is less accurate in describing the molar volume of L₂, a result which can be easily understood considering the data presented in Figure 5.

A prediction of three-phase equilibria of the two following homologues, CO₂–*n*-pentadecane and CO₂–*n*-hexadecane, is presented in Figures 7–10, and as seen, they do not differ from those described before. Although an increase in the molecular weight of the solute approaches the LCEP predicted by LCVM toward the L₁–L₂ UCEP, the model continues to generate phase

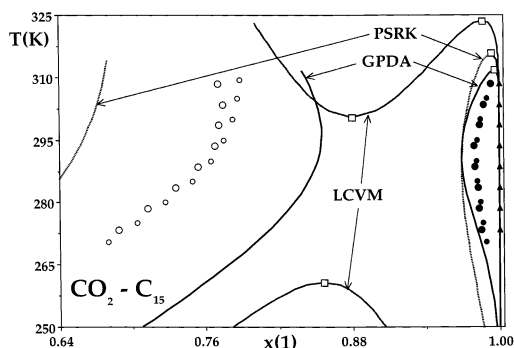


Figure 7. Compositions of LLVE equilibria in the system $\text{CO}_2(1)$ – n -pentadecane(2). Black solid line: data predicted by GPDA. Gray solid line: data predicted by LCV. Black dot line: data predicted by PSRK. \square , calculated critical endpoints. \blacktriangle , experimental data of the vapor phase.³⁹ Experimental data of the CO_2 -rich phase (L_1): \bullet ,³⁸ \bullet .³⁹ Experimental data of the hydrocarbon-rich phase (L_2): \circ ,³⁸ \circ .³⁹

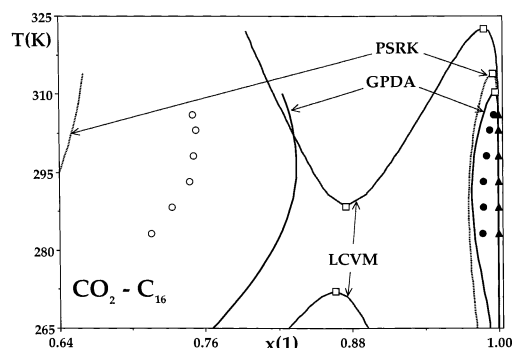


Figure 9. Compositions of LLVE equilibria in the system $\text{CO}_2(1)$ – n -hexadecane(2). Black solid line: data predicted by GPDA. Gray solid line: data predicted by LCV. Black dot line: data predicted by PSRK. \square , calculated critical endpoints. \blacktriangle , experimental data of the vapor phase.³⁹ \bullet , experimental data of the CO_2 -rich phase (L_1).³⁹ \circ , experimental data of the hydrocarbon-rich phase (L_2).³⁹

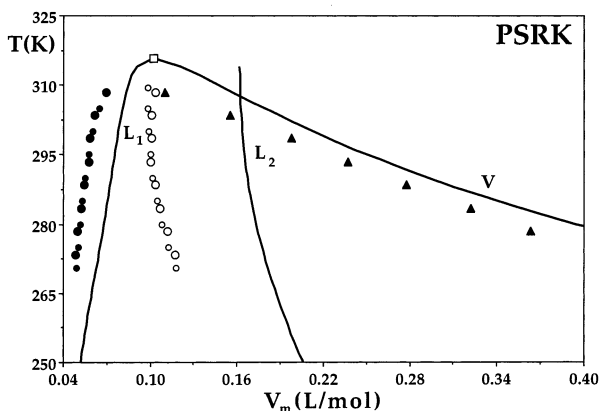
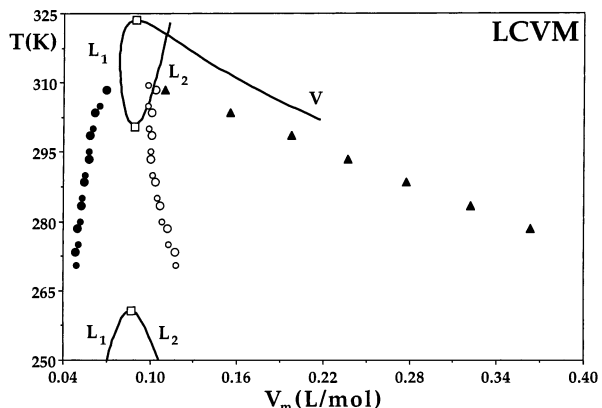
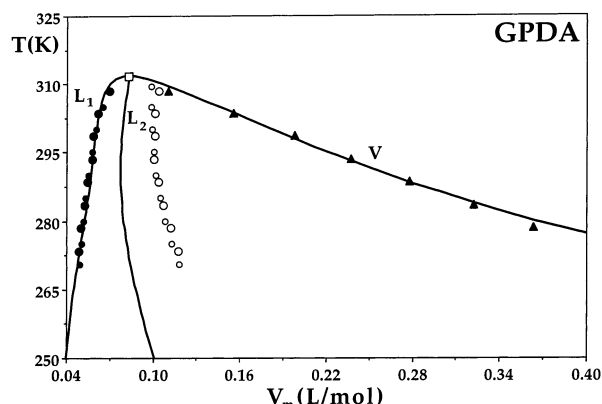


Figure 8. Molar volumes of LLVE equilibria in the system $\text{CO}_2(1)$ – n -pentadecane(2). Black solid line: calculated data. \square , calculated critical endpoints. \blacktriangle , experimental data of the vapor phase.³⁹ Experimental data of the CO_2 -rich phase (L_1): \bullet ,³⁸ \bullet .³⁹ Experimental data of the hydrocarbon-rich phase (L_2): \circ ,³⁸ \circ .³⁹

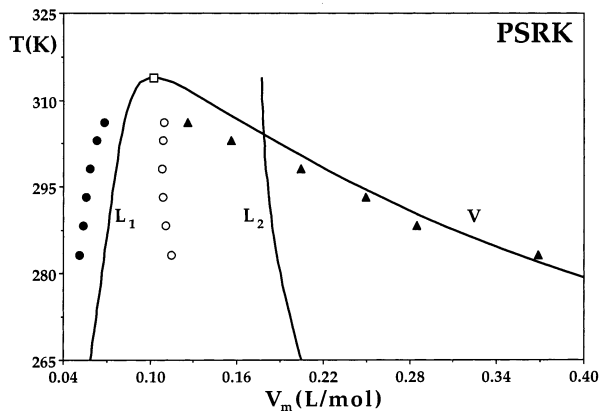
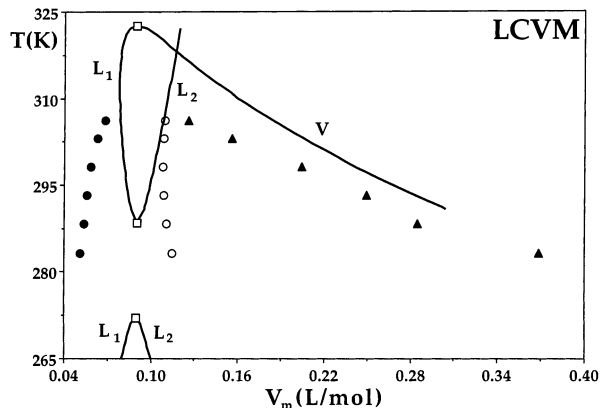
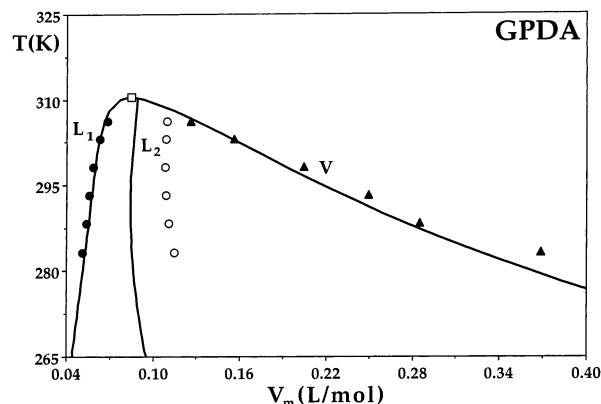


Figure 10. Molar volumes of LLVE equilibria in the system $\text{CO}_2(1)$ – n -hexadecane(2). Black solid line: calculated data. \square , calculated critical endpoints. \blacktriangle , experimental data of the vapor phase.³⁹ \bullet , experimental data of the CO_2 -rich phase (L_1).³⁹ \circ , experimental data of the hydrocarbon-rich phase (L_2).³⁹

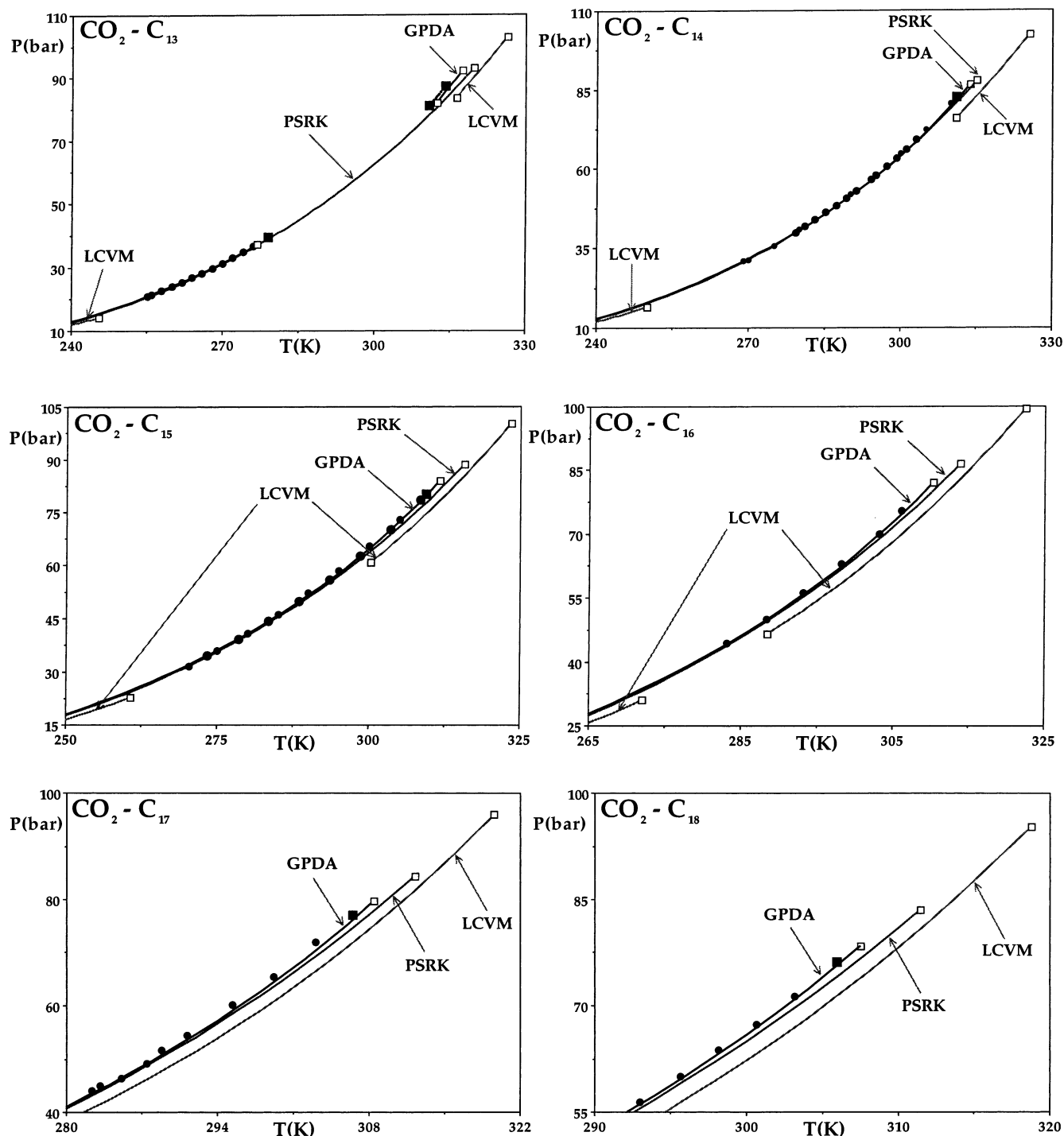


Figure 11. Three-phase equilibria lines in *P*-*T* projection. Black solid line: data predicted by GPDA. Gray solid line: data predicted by LCV. Black dot line: data predicted by PSRK. □, calculated critical endpoints. ■, experimental UCEP.^{38,40} ●, experimental data three-phase data.³⁷⁻⁴⁰

behavior of type IV even for the system CO_2 -*n*-hexadecane. Consequently, LCV completely fails to predict the data. PSRK predicts the composition of L_1 accurately but is unable to describe L_2 and the volumetric properties. GPDA is the best model among the three; it predicts accurately the composition of L_1 and yields precise results for the molar volumes of both L_1 and the vapor phase. In addition, it is more accurate than PSRK in predicting the composition and volume of L_2 .

A clear advantage of GPDA can be also seen in Figure 11 where the three-phase lines are presented in the *P*-*T* projection. It is seen that GPDA precisely predicts the experimental data and slightly overestimates the *K* points. PSRK is also relatively accurate, excepting the system CO_2 -*n*-tridecane, where it fails

to predict the topology of phase behavior. In addition, PSRK is less accurate than GPDA in predicting the *K* points and underestimates the data of heavier homologues. LCV is the less accurate model in describing the data also in the *P*-*T* projection. In addition to predicting the wrong topology up to the system CO_2 -*n*-hexadecane, it also significantly overpredicts the *K* points. As a result, it underestimates the pressures of the three-phase lines, an inaccuracy that increases with the molecular weight of the homologue.

Finally, the data of the heavy homologues (CO_2 -*n*-nonadecane, CO_2 -*n*-eicosane, and CO_2 -*n*-heneicosane) are presented in Figures 12-14. The same behavior patterns are observed for these systems. However, LCV now starts to predict type III

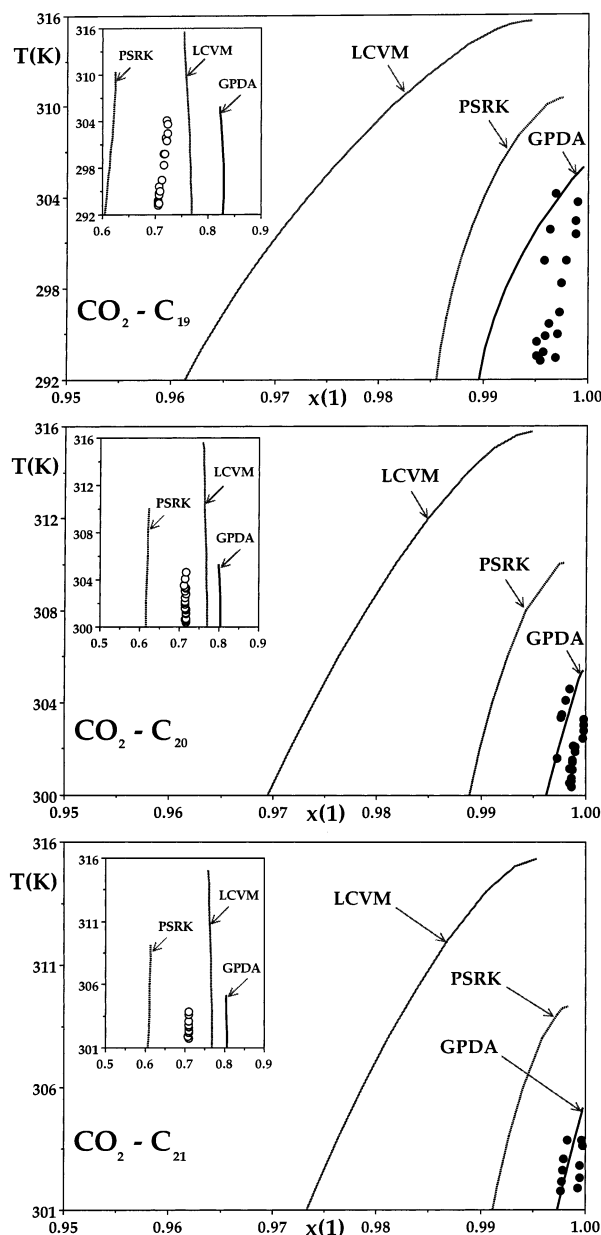


Figure 12. Compositions of LLVE equilibria in the system $\text{CO}_2(1)$ –heavy n -alkanes. Black solid line: data predicted by GPDA. Gray solid line: data predicted by LCVM. Black dot line: data predicted by PSRK. Experimental data of L_1 , \bullet , and L_2 , \circ .⁴¹

phase behavior. Nevertheless, it still continues to be characterized by the already seen inaccuracy. In particular, the prediction of the wrong topology of phase behavior resulted in a serious underestimation of the compositions and densities of L_1 . Yet, although the model now predicts the correct topology of phase behavior, it continues to underestimate the data significantly. In addition, LCVM continues to overpredict the K points, which on one hand occasionally leads to relatively accurate predictions of L_2 and on the other leads to significant deviations from the experimental points in the P – T projection. PSRK is more accurate than LCVM in predicting the composition of L_1 but less accurate in predicting the molar volume of the phase. In addition, PSRK yields better results for the K points and the three-phase data in the P – T projection. Although GPDA continues to yield inaccurate results for L_2 , it is again the most reliable model. In contrast to the two other equations, it precisely predicts the compositions and the molar volumes of L_1 . It also predicts correctly the pressures of three-phase equilibria and

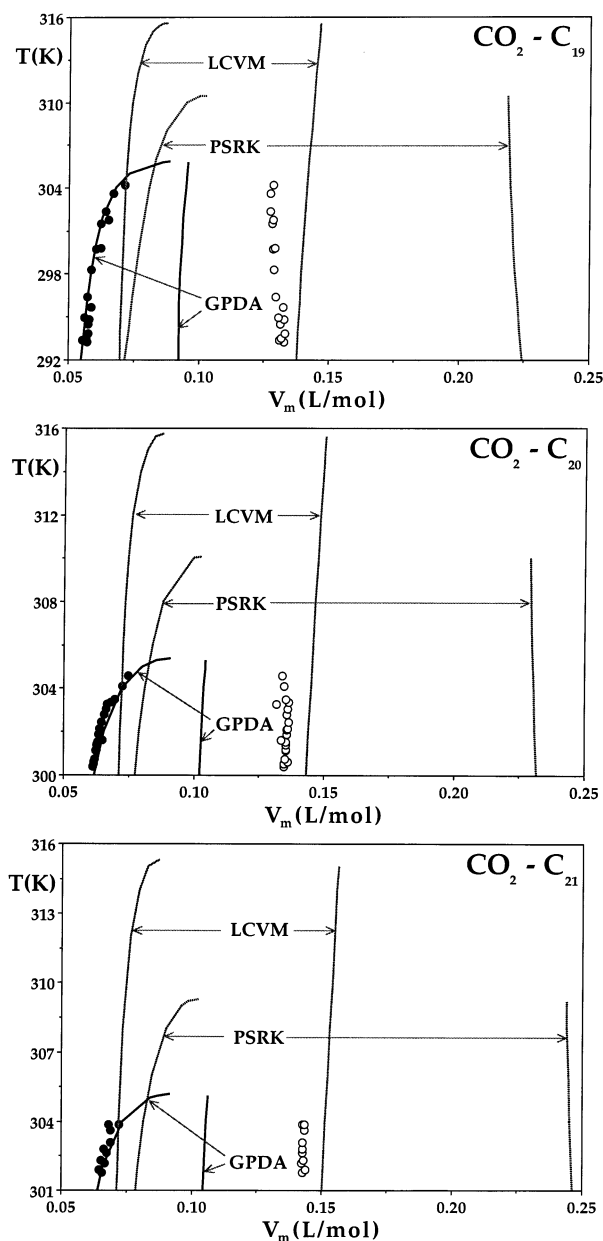


Figure 13. Molar volumes of LLVE equilibria in the system $\text{CO}_2(1)$ –heavy n -alkanes. Black solid line: data predicted by GPDA. Gray solid line: data predicted by LCVM. Black dot line: data predicted by PSRK. Experimental data of L_1 , \bullet , and L_2 , \circ .⁴¹

the K points. These results clearly demonstrate the robustness and the reliability of the semi-predictive approach, which is based not on the local fit of data but on an overall consideration of the entire thermodynamic phase space.

4. Conclusions

In the present study, the possibility of predicting three-phase equilibria without preliminary resource to the experimental data has been examined for the first time. This has been done by implementing the two most successful G^E -based semipredictive models, PSRK and LCVM, and the kIGPD-based semipredictive approach (GPDA) in order to estimate the data of the homologue series carbon dioxide- n -alkanes. GPDA requires the data of only two experimental key points to predict the entire thermodynamic phase space in the complete homologue series. It reveals significant advantages over the G^E -based models, which require a large amount of experimental data in order to achieve

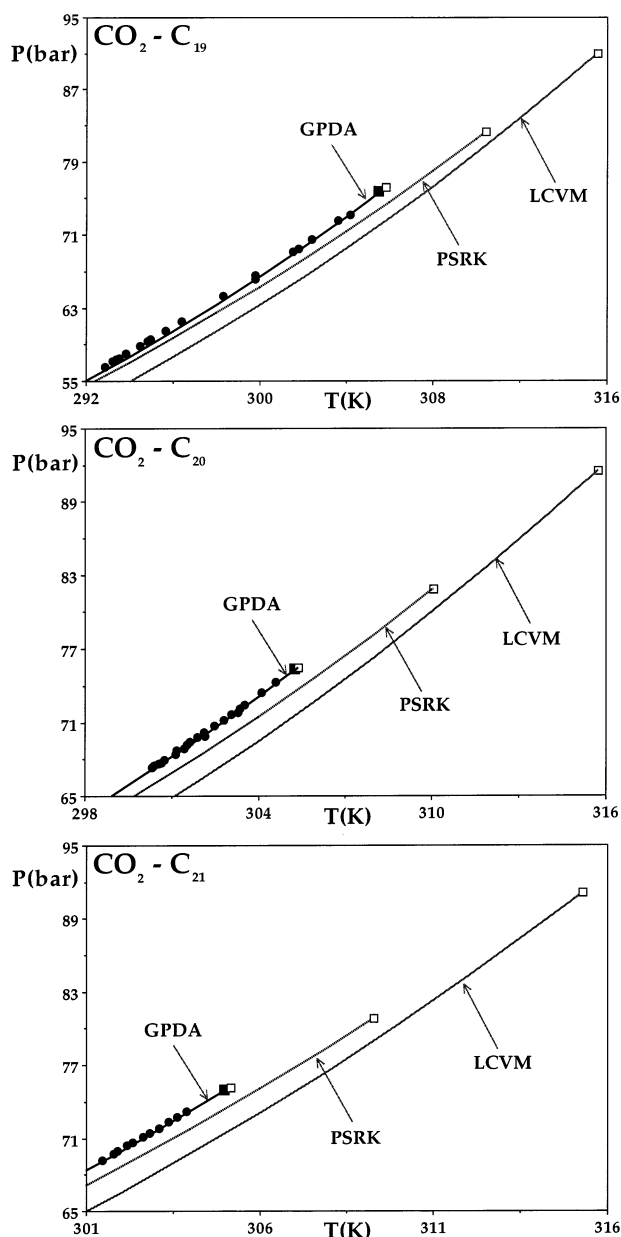


Figure 14. Three-phase equilibria lines in P - T projection in the system $\text{CO}_2(1)$ -heavy n -alkanes. Black solid line: data predicted by GPDA. Gray solid line: data predicted by LCVM. Black dot line: data predicted by PSRK. \square , calculated critical endpoints. \blacksquare , experimental UCEP.⁴¹ \bullet , experimental data three-phase data.⁴¹

predictive ability. The parameters of the LCVM have been evaluated from the data of the homologues considered here. Therefore, this model does not appear here as entirely predictive. In contrast, both PSRK and GPDA do not resource to the pertinent experimental data. The results of the present study can be summarized as follows:

(1) Neglecting parts of the thermodynamic phase space *always* carries a price. LCVM underestimates the critical compositions when attempting to achieve the precise fit of the bubble-point lines. This practice leads to an inaccurate estimation of the critical endpoints, to a failure in predicting the global phase behavior of the whole homologue series, and to a wrong description of the three-phase data.

(2) Although PSRK appears here as an entirely predictive model and it is significantly less accurate than LCVM in describing VLE, it yields somewhat better results for LLVE. Excepting the homologues lighter than CO_2 - n -tetradecane,

where PSRK fails to describe the topology of phase behavior, it is more accurate than LCVM in predicting the compositions of the CO_2 -rich phase, the K points, and the three-phase lines in the P - T projection. Nevertheless, it still gives a rather inaccurate prediction of these data. Moreover, PSRK fails to predict the volumetric data and significantly underestimates the composition of the hydrocarbon-rich phase.

(3) GPDA is clearly superior to PSRK and LCVM in predicting the three-phase data. In contrast to these models, it yields accurate predictions of global phase behavior and the critical endpoints. As a result, it yields an accurate description of the compositions of the CO_2 -rich liquid phase. In addition, the accurate four-parameter EOS used by GPDA allows a precise prediction of the volumetric properties of the vapor and the CO_2 -rich liquid phases. Moreover, GPDA is also exact in predicting the three-phase data in the P - T projection. However, as the other models considered here, GPDA yields an inaccurate modeling of the hydrocarbon-rich phase. Presently, we do not know how to achieve a better description of all three equilibrium phases and the critical lines, without preliminary resource to experimental data of the particular systems.

Acknowledgment. This work was financed by the Israel Science Foundation, Grant No. 340/00 and by FONDECYT, Santiago, Chile (Project 1020340).

Nomenclature

- a = cohesion parameter
- b = covolume
- c, d = attraction density dependence parameters in eq 1
- G^E = excess Gibbs energy
- P = pressure
- R = universal gas constant
- T = temperature
- X = mole fraction of the lighter compound
- V = volume

Greek Letters

- ω = acentric factor

Subscripts

- C = critical state
- M = molar property

Abbreviations

- CPM = critical pressure maximum
- DCEP = double critical end point
- EOS = equation of state
- GPD = global phase diagram
- GPDA = global phase diagram approach
- klGPD = global phase diagram in the k_{12} - l_{12} projection
- LCEP = lower critical end point
- LCVM = linear combination of the Vidal and Michelsen mixing rules
- LLE = liquid-liquid equilibria
- LLLE = liquid-liquid-liquid equilibria
- LLVE = liquid-liquid-vapor equilibria
- PSRK = predictive Soave-Redlich-Kwong group contribution EOS
- SAFT = statistical associating fluid theory EOS
- TCP = tri-critical point
- UCEP = upper critical end point
- UCST = upper critical solution temperature
- VLE = vapor-liquid equilibria

References and Notes

- (1) Deiters, U. K.; Pegg, I. L. *J. Phys. Chem.* **1989**, 90, 6632.
- (2) Jacob, J.; Anisimov, M. A.; Kumar, A.; Agayan, V. A.; Sengers, J. V. *Int. J. Thermophys.* **2000**, 6, 1321.
- (3) Jacob, J.; Anisimov, M. A.; Sengers, J. V.; Oleinikova, A.; Weingärtner, H.; Kumar, A. *Phys. Chem. Chem. Phys.* **2001**, 3, 829.
- (4) Van Konynenburg, P. H.; Scott, R. L. *Philos. Trans. R. Soc. London A* **1980**, 298, 495.
- (5) Gregorowicz, J.; de Loos, Th. W. *Fluid Phase Equilib.* **1996**, 118, 121.
- (6) Soave, G. *Chem. Eng. Sci.* **1972**, 27, 1197.
- (7) Gregorowicz, J.; de Loos, Th. W. *Ind. Eng. Chem. Res.* **2001**, 40, 444.
- (8) Peng, C. J.; Robinson, D. B. *Ind. Eng. Chem. Fundam.* **1976**, 15, 59.
- (9) Orbey, N.; Sandler, S. I. *AIChE J.* **1990**, 40, 1203.
- (10) Huang, S. H.; Radosz, M. *Ind. Eng. Chem. Res.* **1991**, 30, 1994.
- (11) Polishuk, I.; Wisniak, J.; Segura, H.; Yelash, L.; Kraska, T. *Fluid Phase Equilib.* **2000**, 172, 1.
- (12) Polishuk, I.; Wisniak, J.; Segura, H. *Chem. Eng. Sci.* **2001**, 56, 6485.
- (13) Holderbaum, T.; Gmehling, J. *Fluid Phase Equilib.* **1991**, 70, 251.
- (14) Boukouvalas, C.; Spiliotis, N.; Coutisikos, P.; Tzouvaras, N.; Tassios, D. *Fluid Phase Equilib.* **1994**, 92, 75.
- (15) Myers, A. L.; Prausnitz, J. M. *Ind. Eng. Chem. Fundam.* **1965**, 4, 209.
- (16) Mathias, P. M.; Copeman, T. W. *Fluid Phase Equilib.* **1983**, 13, 91.
- (17) Dahl, S.; Michelsen, M. L. *AIChE J.* **1990**, 36, 1829.
- (18) Fischer, K.; Gmehling, J. *Fluid Phase Equilib.* **1996**, 121, 185.
- (19) Gmehling, J.; Jiding, L.; Fischer, K. *Fluid Phase Equilib.* **1997**, 141, 113.
- (20) Horstmann, Fischer, K.; Gmehling, J. *Fluid Phase Equilib.* **2000**, 167, 173.
- (21) Polishuk, I.; Stateva, R.; Wisniak, J.; Segura, H. *Can. J. Chem. Eng.* **2002**, in press.
- (22) Polishuk, I.; Wisniak, J.; Segura, H. *Chem. Eng. Sci.* **2002**, submitted.
- (23) Li, J.; Fischer, K.; Gmehling, J. *Fluid Phase Equilib.* **1998**, 143, 71.
- (24) Zhong, C.; Masuoka, H. *J. Chem. Eng. Jpn.* **1996**, 29, 315.
- (25) Yang, Q.; Zhong, C. *Fluid Phase Equilib.* **2001**, 192, 103.
- (26) Magoulas, K.; Tassios, D. *Fluid Phase Equilib.* **1990**, 56, 119.
- (27) Huron, M.-J.; Vidal, J. *Fluid Phase Equilib.* **1979**, 3, 255.
- (28) Kontogeorgis, G. M.; Vlamos, P. M. *Chem. Eng. Sci.* **2000**, 55, 2351.
- (29) Polishuk, I.; Wisniak, J.; Segura, H. *Phys. Chem. Chem. Phys.* **2002**, 4, 879.
- (30) Polishuk, I.; Wisniak, J.; Segura, H.; Kraska, T. *Ind. Eng. Chem. Res.* **2002**, 41, 4414.
- (31) Polishuk, I.; Wisniak, J.; Segura, H. *Chem. Eng. Sci.* **2000**, 55, 5705.
- (32) Polishuk, I.; Wisniak, J.; Segura, H. *Phys. Chem. Chem. Phys.* **1999**, 1, 4245.
- (33) Daubert, T. E.; Danner, R. P.; Sibul, H. M.; Stebbins, C. C. *Physical and Thermodynamic Properties of Pure Chemicals. Data Compilations*; Taylor & Francis: Bristol, PA, 1989–2002.
- (34) Danesh, A.; Todd, A. C.; Somerville, J.; Dandekar, A. *Chem. Eng. Res. Des.* **1990**, 68, 325.
- (35) Gasem, K. A. M.; Dickson, K. B.; Dulcamara, P. B.; Nagarajan, N.; Robinson, R. L., Jr. *J. Chem. Eng. Data* **1989**, 34, 191.
- (36) Enick, R.; Holder, G. F.; Morsi, B. I. *Fluid Phase Equilib.* **1985**, 22, 209.
- (37) Fall, D. J.; Lucks, K. D. *J. Chem. Eng. Data* **1985**, 30, 276.
- (38) Hottovy, J. D.; Lucks, K. D.; Kohn, J. P. *J. Chem. Eng. Data* **1981**, 26, 256.
- (39) Van der Steen, J.; de Loos, Th. W.; de Swaan Arons, J. *Fluid Phase Equilib.* **1989**, 51, 353.
- (40) Iwade, S.; Katasumura, Y.; Ohgaki, K. *J. Chem. Eng. Jpn.* **1993**, 26, 74.
- (41) Fall, D. J.; Fall, J. L.; Lucks, K. D. *J. Chem. Eng. Data* **1985**, 30, 82.